Dual-Readout Calorimetry for High-Quality Energy Measurements

Progress Report

Presented by:

Dr. Richard Wigmans[1]

on behalf of the RD52 (DREAM) Collaboration

CERN-SPSC-2016-014 / SPSC-SR-182
18/03/2016

19 April 2016

[1]Contact person. Tel. [806] 834 6283, FAX [806] 742 1182, E-mail: wigmans@ttu.edu

1 Introduction

On August 31, 2011, the CERN Research Board decided to accept the DREAM Collaboration's detector R&D proposal [1] and included it as project RD52 in its official scientific program. This document constitutes the fifth RD52 progress report. In this report, we describe our activities since the last time we reported to the SPS Committee (April 14, 2015 [2]), as well as our future plans.

Since our last report to the SPSC, two new papers with results from our 2014 test beam campaign were published. These results were presented last year in the April 14 SPSC meeting. At the end of 2015, we were allocated 2 weeks of beam time in our usual location at the end of the H8 beam line. We used this time to collect some new data with the two fiber calorimeters described in our previous annual SPSC report. We are in the process of analyzing these data, and expect to submit two papers describing the new results later this year.

We are currently preparing for a new round of experimental data taking in 2016, using our existing calorimeters. We also hope to test some new copper based calorimeter modules, which we plan to construct in Ames, Iowa. In the past year, the latest RD52 results have been presented at a number of colloquia and seminars. They were also featured at the Elba conference in May 2015. The talks, as well as all publications in the context of this project, can be found at the RD52 website:
http://highenergy.phys.ttu.edu/dream/results/talks/talks.html

Details about our various past, current and planned activities are given in the next sections.

2 New results

The results of our beam tests in 2014 have been summarized in the following recent publications:

- *The small-angle performance of a dual-readout fiber calorimeter*,
  A. Cardini *et al.*, Nucl. Instr. and Meth. in Phys. Res. **A808** (2016) 41 - 53.

- *New Results from the RD52 Project*,
  R. Wigmans, accepted for publication in Nucl. Instr. and Meth.,
  DOI: 10.1016/j.nima.2015.09.069

These results were presented at last year's SPSC meeting, and are also featured in Reference [2].

2.1 Characteristics of the light produced in the dual-readout calorimeter

The performance of hadron calorimeters is typically strongly dominated, and negatively affected, by the effects of fluctuations in the electromagnetic (em) shower fraction, $f_{\rm em}$. Our approach to eliminate the effects of such fluctuations is to *measure* $f_{\rm em}$ for each event. It turns out that the Čerenkov mechanism provides unique opportunities in this respect, since calorimeters that use Čerenkov light as signal source are, for all practical purposes, only responding to the em fraction of hadronic showers. By comparing the relative strengths of the signals representing the visible deposited energy (dE/dx) and the Čerenkov light produced in the shower

absorption process, the em shower fraction can be determined and the total shower energy can be reconstructed using the known e/h value(s) of the calorimeter. This is the essence of what has become known as *dual-readout* calorimetry.

In the RD52 dual-readout calorimeter, signals are generated in scintillating fibers, which measure the deposited energy, and in clear plastic fibers, which measure the charged relativistic shower particles, by means of the Čerenkov light generated by these. A large number of such fibers are embedded in a metal absorber structure. This detector is longitudinally unsegmented, the fibers are oriented in *approximately* the same direction as the particles to be detected.

In previous studies, we found that the em energy resolution deteriorated when the electrons or photons entered the calorimeter almost parallel to the optical fibers, *but only for the scintillation signals, not for the Čerenkov ones* [3]. This was explained from the fact that the early component of em showers (*i.e.* before the shower maximum is reached) is extremely collimated. When an electron enters this calorimeter parallel to the fibers, the scintillation signal from the early shower component strongly depends on the impact point, *i.e.* inside a fiber or in between fibers, and this dependence leads to an energy independent contribution to the em energy resolution. This early, extremely collimated shower component does *not* contribute significantly to the Čerenkov signals, because the (highly directional) Čerenkov light it generates falls outside the numerical aperture of the fibers. Therefore, the em energy resolution is not subject to the aforementioned energy independent term. As a matter of fact, at very small angles of incidence the Čerenkov energy resolution was actually measured to be substantially better than that measured with the scintillation signals, despite the much smaller Čerenkov light yield and the correspondingly larger fluctuations in the number of signal quanta. The explanation of the small angle effects described above was *more or less* confirmed by GEANT4 based Monte Carlo simulations of em shower development in our calorimeter [3, 4], even though discrepancies remained concerning some of the details.

In these new studies, we tried explicitly to measure the differences between the contributions of the early em shower component to the two types of calorimeter signals. The calorimeter was rotated over 90 degrees and placed perpendicular to the beam of incoming particles in these measurements. This geometry also made it possible to measure some other important experimental features of the calorimeter, such as the light attenuation in the two types of fibers, the reflection coefficient of the mirrored upstream ends of the Čerenkov fibers, and the possibilities to separate the direct and reflected components of the Čerenkov light.

For these particular studies, we used a beam of 80 GeV positrons, which were steered into a module of the RD52 fiber calorimeter. A system of auxiliary detectors was used to select the desired beam particles that entered the calorimeter in a well defined, small area.

The calorimeter module used for these studies consisted of a copper absorber matrix, 2.5 m long, with a cross section of 9.2×9.2 cm^2. It was subdivided into four towers ($4.6\times4.6\times250$ cm^3), and each tower contained 1024 plastic optical fibers (diameter 1.0 mm, equal numbers of scintillating and clear plastic fibers). For the measurements described in this report, only one of these four towers was used. This tower produced two signals, a scintillation signal and a Čerenkov signal, which were detected by separate PMTs. Because of the need for signal speed in these studies, we chose Microchannel Plate PMTs for this purpose[1], since these are faster than

[1] 2" $\times$ 2" Planacon XP85012 (scintillation signal), XP85112 (Čerenkov signal), produced by Photonis.

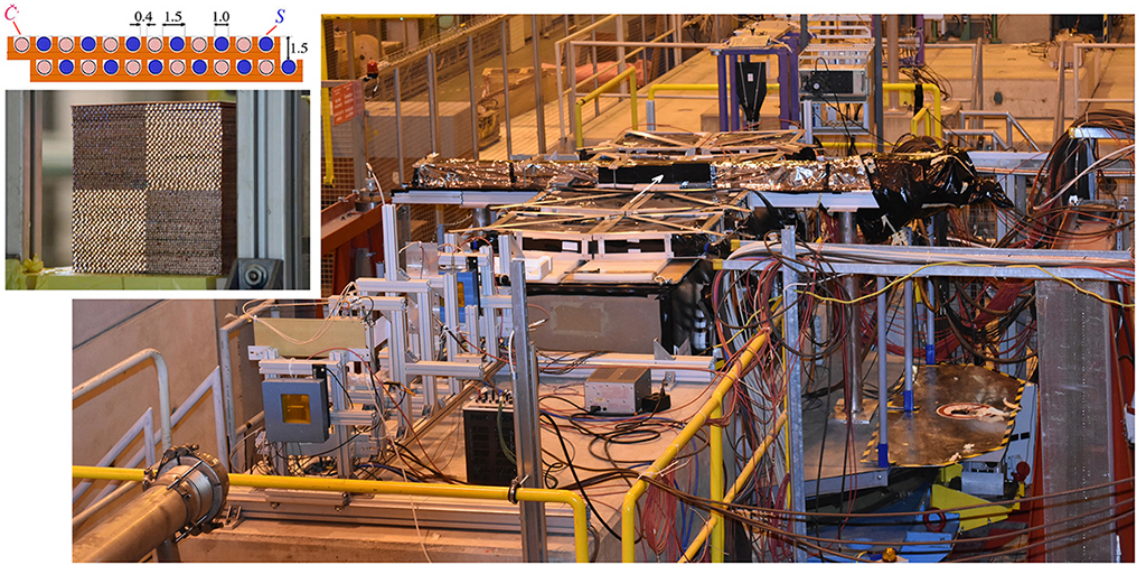

Figure 1: Experimental setup in the H8 beam of the SPS at CERN. The calorimeter module is installed perpendicular to the beam line, wrapped in foil. The impact point of the beam particles, which arrive through the tube visible in the bottom left corner, is indicated by a white arrow. The black material into which the particles enter is lead installed directly upstream of the calorimeter module. The mirrored fiber ends are located on the left hand side in this picture (shown in closeup in the insert), and the PMT readout on the right hand side. The insert also shows the way in which the two types of fibers are embedded in the copper matrix.

the standard dynode based PMTs we had used in the past. An important reason for the need for fast signals was the fact that the upstream ends of the clear plastic fibers (in which the Čerenkov light was produced) were aluminized, and we wanted to see a clear separation between the direct and the reflected light components contributing to the Čerenkov signals.

In the studies we performed earlier with this calorimeter and its predecessors of the dual-readout type [2], the calorimeter was always oriented such that the incoming particles travelled in (approximately) the same direction as the fibers. However, for the measurements performed for the present studies the calorimeter module was rotated by 90 degrees, so that the beam particles entered the detector (approximately) perpendicular to the fiber direction. Figure 1 shows the experimental setup in the H8 beam at the CERN SPS. In this way, the effective thickness of the calorimeter tower is only 1.8 radiation lengths (X_0). By placing absorber material directly in front of the calorimeter, this tower probed the calorimeter signals produced in a certain $1.8X_0$ thick slice, located at a depth determined by the amount of absorber material placed upstream (visible as black blocks placed in the way of the particle beam, which is indicated by the white arrow in Figure 1). The insert of the figure shows a closeup picture of the open end of the calorimeter, the 4 towers of which it consists are made visible by means of light shone in from the other (PMT) end. The insert also shows the detailed structure of the calorimeter, with alternating scintillating and Čerenkov fibers embedded in the copper matrix.

The time structure of the calorimeter signals was recorded by means of a digitizer based on the DRS-IV chip [5]. This chip offers both a very fast sampling rate and a wide buffer. We used a 32-channel CAEN V1742 VME unit, which is based on this chip, for our purpose. The sampling

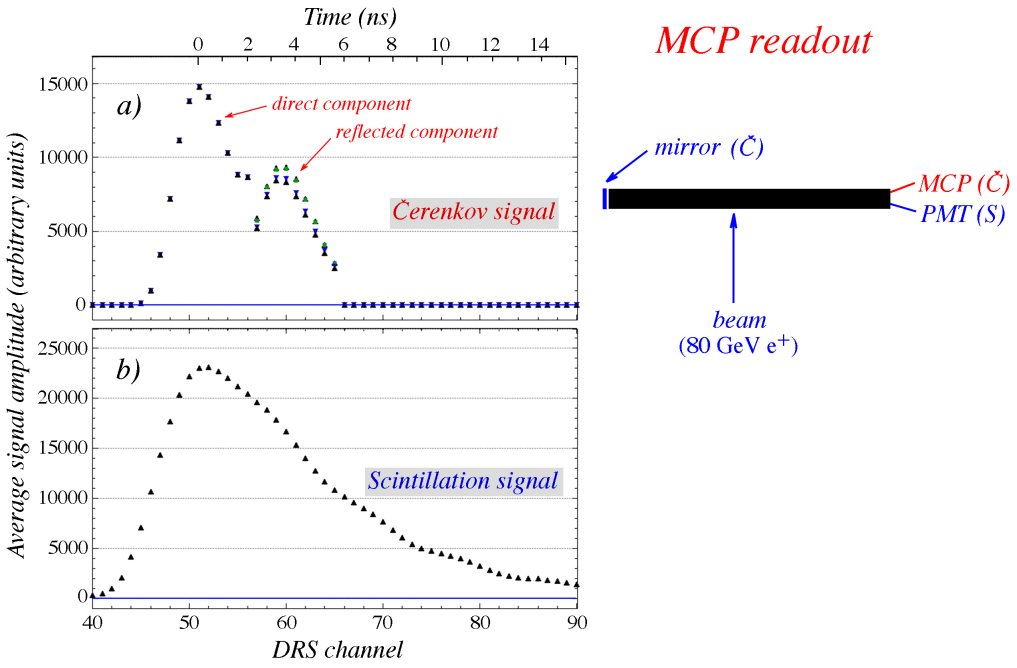

Figure 2: Typical time structure of the Čerenkov (a) and scintillation (b) signals measured for 80 GeV positrons entering the calorimeter perpendicular to the fibers. The impact point was located at 29.5 cm from the mirrored front end of the fibers. The direct and reflected light components of the Čerenkov signals are clearly separated.

frequency was set at 2.5 Gs/s, which gave us 1024 data points, each separated by 0.4 ns, for every signal. To illustrate the type of information obtained from the DRS measurements, we show in Figure 2 the average time structure of the Čerenkov (a) and scintillation (b) signals recorded when the 80 GeV e^+ beam entered the calorimeter module perpendicularly ($\phi = 0$) at a distance of 29.5 cm from the front face of the module. Because of the limitations of our experimental area, this was as close as we could get to the aluminized front face. The Čerenkov signals clearly show the direct and reflected components, which are still clearly distinguishable despite the fact that the difference in arrival time is only slightly more than 3 ns[2]. The scintillation signal is clearly less fast than the Čerenkov ones, because of the decay time of the scintillating dye. Because of the fact that the upstream end of the scintillating fibers was not aluminized, no reflected signals are observed.

A similar figure was made for all measurements of this type made at different impact points (x values). The results, plotted in Figure 3, show that the measured time differences between the direct and reflected components of the Čerenkov signals are well described by a linear fit, which crosses zero at the front edge of the module. The slope of this line gives us the speed at which the Čerenkov light travels through the plastic fibers: 21.0 $\pm$ 0.2 cm/ns. This is in good agreement with c/n, if one takes into account the fact that the light does not travel in a straight

[2]The fact that multiple data sets are plotted in this figure is a consequence of different procedures that were used to establish the base line of the signals. The variation between the different data sets is interpreted as a systematic uncertainty in the results.

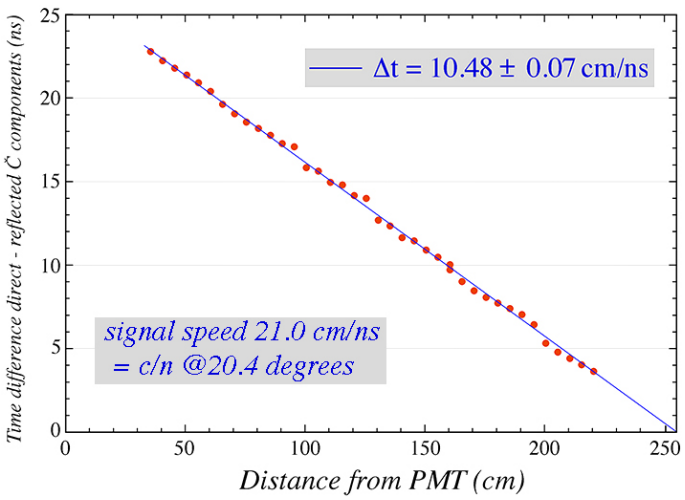

Figure 3: The time difference between the direct and reflected components of the Čerenkov light generated by 80 GeV positrons entering the calorimeter perpendicular to the fibers, as a function of the distance between the impact point and the PMTs.

line, but at an angle $\lesssim 20.4°$, the angle of total internal reflection in the clear plastic fibers[3]

The measurements also allowed us to obtain information about some important practical aspects of the calorimeter under study, and in particular the light attenuation in both types of fibers and the reflection coefficient of the aluminized upstream end of the Čerenkov fibers. These characteristics were of course also measured prior to construction with radioactive sources generating signals in individual fibers. However, these measurements were not necessarily representative for the detection of high energy showers in a calorimeter containing thousands of fibers. The calorimeter was oriented perpendicular to the beam line and located directly behind 2.5 cm of lead absorber[4] for these measurements. The scintillation signal was measured to decrease by $\sim 30\%$ over a distance of 1 m. A fit to the experimental data gave an attenuation length of about 3 m, which is shorter than the 5 m measured in lab tests. The Čerenkov light was much less attenuated, presumably because the self absorption that occurs in the scintillating dye does not play a role in this case. Figure 4a shows the average Čerenkov signals as a function of the impact point of the beam particles. The figure shows both the data points for the direct and the reflected Čerenkov light signals, as well as the sum of both signals. The latter was almost constant over the 1.4 m range of the measurements, consistent with the lab measurements (15 m attenuation length).

These data also made it possible to estimate the reflection coefficient of the aluminized upstream ends of the Čerenkov fibers. Figure 4b shows the ratio of the reflected and direct Čerenkov signals, as a function of the distance to the front face of the calorimeter module. A linear fit of the data points extrapolates to a ratio of 0.62 ± 0.05 at the front face, and this is thus the effective reflectivity of the mirrors.

[3]The indices of refraction of the core and cladding of these fibers are 1.49 and 1.40, respectively.

[4]This was needed to increase the size of the signals, which were extremely small in the very first radiation lengths of the developing showers.

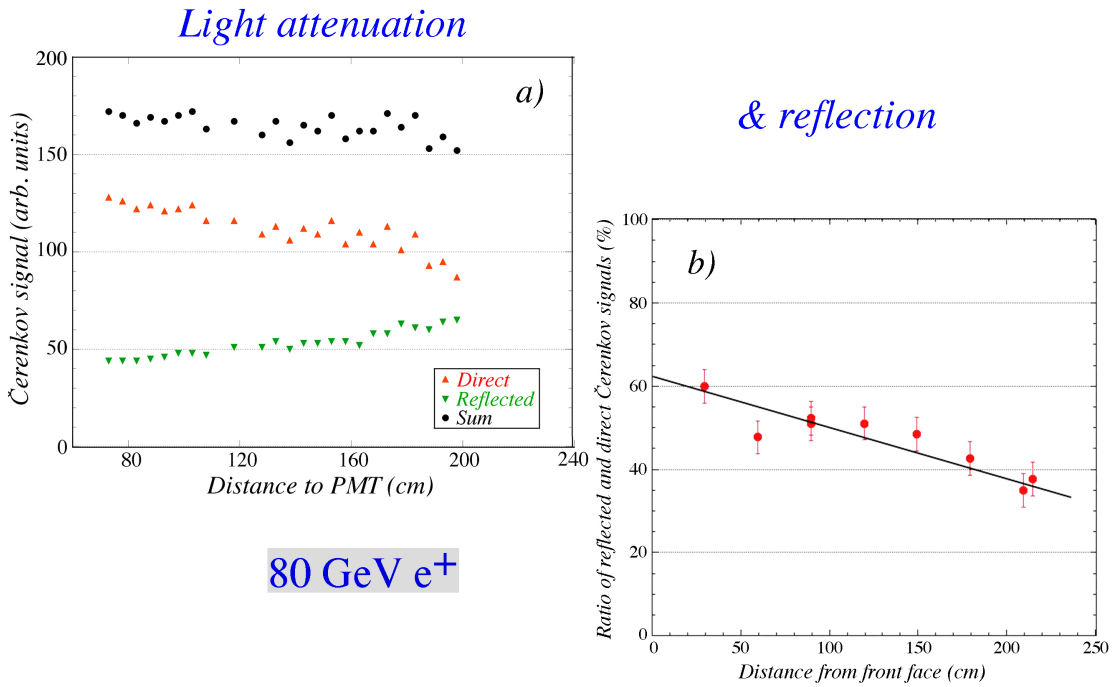

Figure 4: The average Čerenkov signals generated by 80 GeV positrons entering the calorimeter perpendicular to the fibers, as a function of the distance between the impact point of the beam and the PMT. Results are given separately for the direct and the reflected light components, and for the sum of both signals (a). The ratio of the reflected and direct components of the Čerenkov signals, as a function of the distance from the aluminized front ends of the clear plastic fibers (b).

As stated in the introduction, our main goal was to study differences between the early shower components measured with the two types of signals. When the beam particles entered the calorimeter perpendicularly, they traversed an amount of material that represents only about 1.8 radiation lengths, and they deposited only a small fraction of their energy in the traversed tower. That fraction, and thus the recorded signals, could be increased by placing additional absorber material upstream of the calorimeter. For example, if that upstream material was a standard lead "brick" with a thickness of 5 cm (8.9 X_0), then the calorimeter signal measured the shower energy deposited at a depth ranging from 8.9 - 10.7 X_0. By placing blocks of lead with different thicknesses directly upstream of the calorimeter, the measured calorimeter signals became indicative for the shower energy deposited in 1.8 X_0 thick slices at different depths inside the calorimeter.

Figure 5 shows the average signal measured in the scintillating fibers, as a function of the amount of lead installed upstream of the calorimeter. The thickness of this lead is given in the top scale. The bottom scale indicates the average depth of the calorimeter slice probed in these various measurements, in units of radiation lengths. The horizontal error bars represent the thickness of that depth slice. The experimental data points are well described by a smooth curve that represents a typical electromagnetic shower profile for 80 GeV positrons in lead, the main absorber material in this case. The curve rises initially almost linearly with increasing depth, reaches a maximum at a depth of $\sim 8X_0$ and decreases gradually beyond that point.

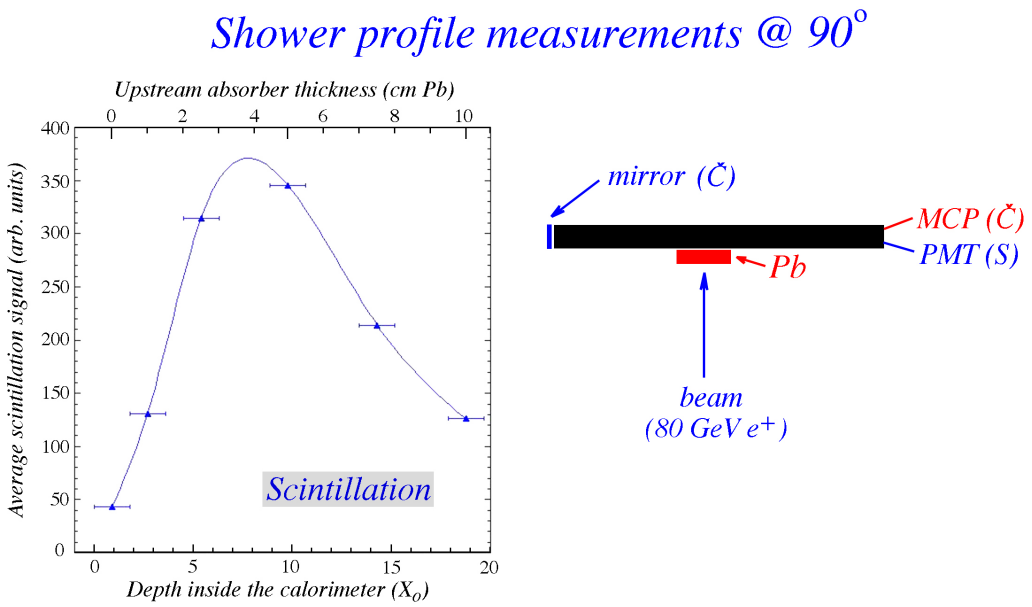

Figure 5: The average scintillation signal generated by 80 GeV positrons entering the calorimeter perpendicular to the fibers at a distance of 100 cm from the PMT, as a function of the thickness of the lead installed directly upstream of the calorimeter.

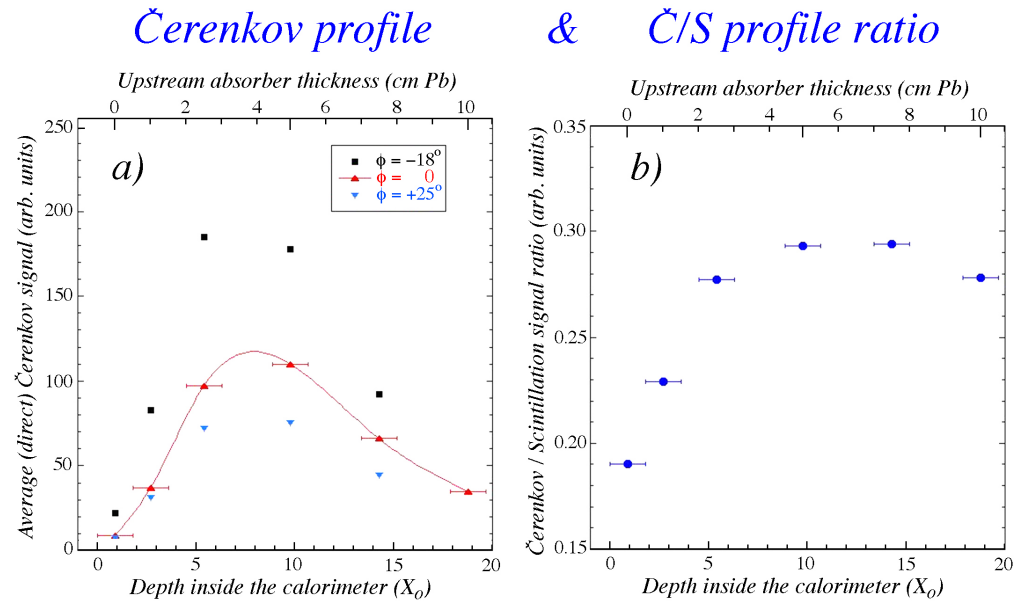

Figure 6: The average (direct) Čerenkov signal generated by 80 GeV positrons entering the calorimeter at a distance of 100 cm from the PMT, as a function of the thickness of the lead installed directly upstream of the calorimeter. Results are given for perpendicular incidence ($\phi = 0$), as well as for angles ϕ of -18° and +25°, respectively (a). The ratio of the Čerenkov and scintillation signals measured for perpendicular incident 80 GeV positrons (b).

Similar information is shown in Figure 6a, for the average Čerenkov signals. Only the direct, non-reflected portion of the signals was considered for this purpose. Apart from the measurements performed for the perpendicular orientation of the calorimeter module ($\phi = 0$), the figure also shows the results obtained for the angles $\phi = -18^\circ$ and $\phi = +25^\circ$. A comparison between the three data sets illustrates the sensitivity of the Čerenkov response to the angle of incidence of the beam particles. The maximum response to the direct Čerenkov light is expected at $\phi = -42^\circ$, when the axis of the Čerenkov cone coincides with the fiber axis[5].

As in the case of the scintillation signals, the shower profile measured for perpendicular incidence of the beam particles reaches a maximum at a depth of $\sim 8X_0$. Interestingly, this maximum is reached somewhat earlier for the other data sets. This can be understood from the fact that the effective depth of the lead installed upstream of the calorimeter module is somewhat larger when the beam traverses this lead at an angle $\phi \neq 0$, since the lead was rotated together with the module.

We now turn our attention to the crucial question that inspired these experiments: To what extent is the angular distribution of the Čerenkov light produced in the early stages of the shower development responsible for the fact that no constant term was observed in the em energy resolution measured with the Čerenkov signals? To answer that question, we examined the ratio of the Čerenkov and scintillation signals as a function of the depth inside the calorimeter at which these signals were generated. The result is shown in Figure 6b. It turns out that this ratio is more or less constant for depths $\gtrsim 5X_0$, *i.e.* beyond the shower maximum. However, in the early stages of the shower development, the Čerenkov signals are anomalously small, compared to the scintillation ones. Since the scintillation light is emitted isotropically, this difference must be a consequence of the non-isotropic directionality of the Čerenkov light emitted in the early stages of the shower development.

A paper containing these and some other results of these MCP tests is in preparation, and will later this year be submitted to Nuclear Instruments and Methods for publication.

- *Characteristics of the light produced in a dual-readout fiber calorimeter*, S. Lee *et al.*, to be submitted to Nucl. Instr. and Meth.

2.2 The hadronic performance of the dual-readout fiber calorimeter

The second part of our experimental program in 2015 concerned measurements of the hadronic performance of the 9-module lead-fiber calorimeter we built. This detector is clearly to small to fully contain the hadronic showers, the average lateral leakage amounts to 15-20%, depending on the energy of the incoming hadron, and event-to-event fluctuations in that leakage are a dominant contribution to the energy resolution. Our experimental program concentrated on two issues:

1. To what extent can the very crude system of leakage counters that we had installed around the calorimeter measure these event-to-event fluctuations and improve the measured energy resolution?

[5]The Čerenkov angle is given by $\arccos\theta_C = 1/n$, with the index of refraction $n = 1.49$, and $\phi = \theta_C - 90^\circ$.

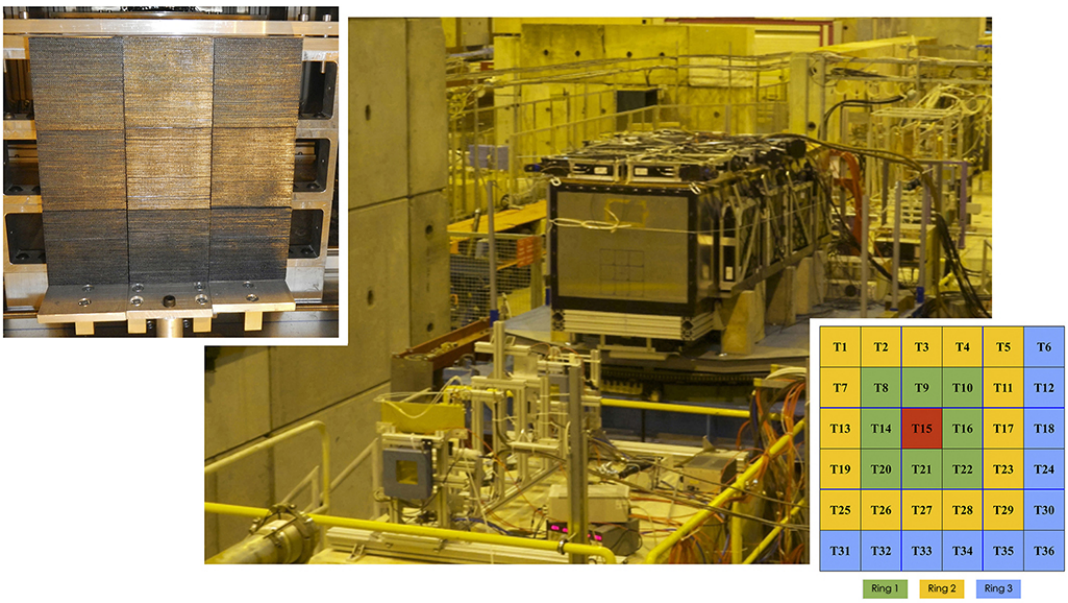

Figure 7: Experimental setup in the H8 beam of the SPS at CERN. The calorimeter is installed inside a light tight box, surrounded on 4 sides by 20 modular leakage counters. The entire setup is installed on a movable table, which allows the impact point and the incident angle of the beam particles to be chosen as needed. The beam particles arrive through the tube visible in the bottom left corner, and pass through several beam defining elements upstream of the calorimeter. The left insert shows a picture of the front face of the calorimeter, which consists of a 3×3 matrix of modules. The right insert shows the tower structure, one central tower surrounded by two complete rings and an incomplete one.

2. Can we separate pions and protons in the H8 beam, and measure the dual-readout calorimeter performance separately for these particles?

For these particular studies, we used secondary or tertiary beams derived from the 400 proton beam delivered by the CERN Super Proton Synchrotron. These particle beams were steered through the H8 beam line into the RD52 fiber calorimeter. Figure 7 shows the experimental setup. The fiber calorimeter used for these is modular, and uses lead as the absorber material. Each module is 2.5 m long (10 $\lambda_{\rm int}$), and has a cross section of 9.2×9.2 cm^2. Its fiducial mass is 150 kg. Each module consists of four towers (4.6×4.6×250 cm^3), and each tower contains 1024 plastic optical fibers (diameter 1.0 mm, equal numbers of scintillating and clear plastic fibers). Each tower produced two signals, a scintillation signal and a Čerenkov signal, which were detected by separate PMTs[6]. The sampling fraction for minimum ionizing particles in this calorimeter, both for the scintillation and for the Čerenkov sampling structure, is 5.3%.

Measurements of the radial shower profile showed that the showers initiated by high-energy pions were, on average, contained at the level of 80-85% in this structure. In order to detect this shower leakage, the calorimeter was surrounded by large slabs of plastic scintillator (50×50×10 cm^3, mass 25 kg). Twenty such counters were used in these tests. They can be seen in Figure 7 on the top, the bottom and the right hand side of the box containing the calorimeter. Since em showers were contained to better than 99% in this calorimeter, shower leakage was not an

[6]Hamamatsu R8900, 10-stage.

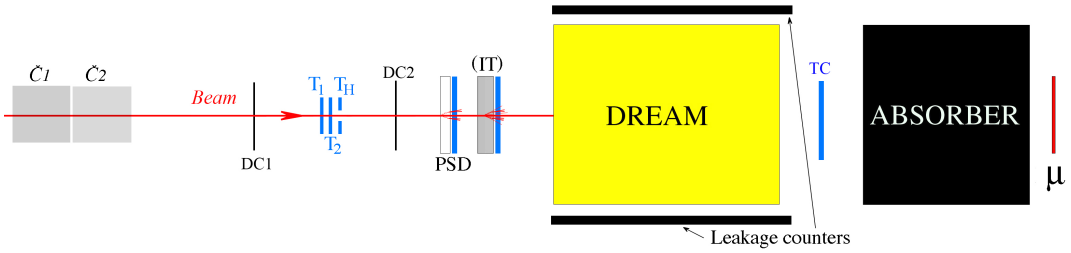

Figure 8: Schematic layout of the experimental setup (not to scale). Shown are the threshold Čerenkov counters (Č), the drift chambers (DC), the trigger counters (T), the preshower detector (PSD), the Interaction Target (IT), the calorimeter surrounded by leakage counters, the Tail Catcher (TC) and the muon counter (μ).

issue for electrons and photons. The experimental setup contained also a number of auxiliary detectors, which were intended to limit and define the effective size of the beam spot, to determine the identity of individual beam particles, and to measure their trajectory. Figure 8 shows a schematic overview of the beam line, in which the positions of these auxiliary counters are indicated (not to scale).

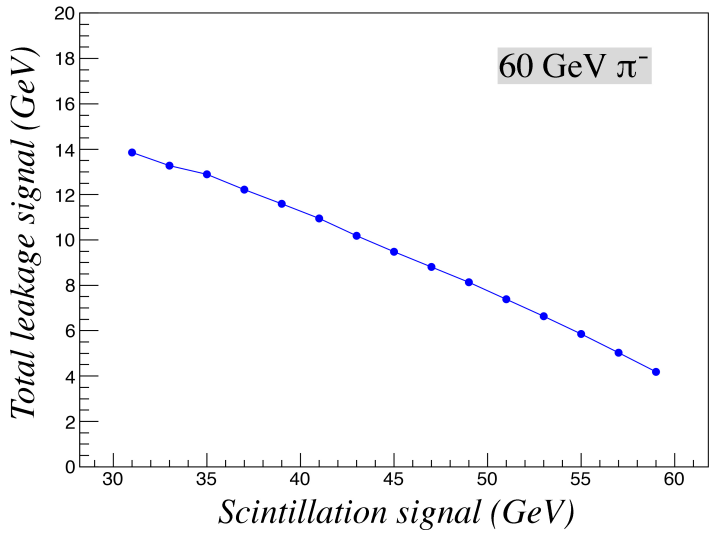

Figure 9: Relationship between the average signals from 60 GeV π^- showers measured in the scintillation channels of the calorimeter and in the array of leakage counters.

In order to study the effectiveness of the described leakage counters, we first studied the correlation between the signals from these counters and the scintillation signals from the fiber calorimeter. The result, shown in Figure 9 for 60 GeV π^-, indicates that there is indeed a good anti-correlation between the *average* signals. However, the resolution improvement depends of course on the event-by-event anti-correlation. Yet, the counters turned out to be indeed somewhat effective in that respect.

An extreme example of this effectiveness is shown in Figure 10, in which the signal distribution for all events (Figure 10a) is compared with the signal distribution for the events in which *no* shower leakage was observed, *i.e.* the (small fraction of the) events that were entirely

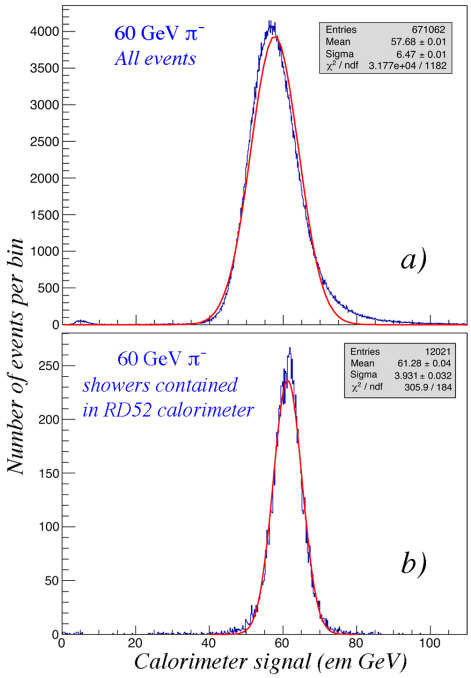

Hadron tests Pb module

Energy resolution hadrons is dominated by

- *Lateral leakage fluctuations*
- *Light attenuation (S)*

Figure 10: Total signal distributions for 60 GeV π^-, corrected with the dual-readout method. Shown are the distributions for all events (a) and for events that were completely contained inside the calorimeter, *i.e.* for which no energy leakage was measured in the leakage counters (b).

contained in the fiber calorimeter. The latter distribution exhibits an energy resolution that is about a factor of two better, and is in addition well described by a Gaussian function.

These, and all other signal distributions shown in this report, were obtained with the standard dual-readout correction procedure. By measuring simultaneously the visible deposited energy (dE/dx) and the Čerenkov light generated in the shower absorption process, one can determine $f_{\rm em}$ *event by event* and thus eliminate (the effects of) its fluctuations. The correct hadron energy can be determined from a combination of both signals. This principle was first experimentally demonstrated by the DREAM Collaboration [6], with a Cu/fiber calorimeter. Scintillating fibers measured dE/dx, quartz fibers the Čerenkov light. The response ratio of these two signals is related to $f_{\rm em}$ as

$$\frac{C}{S} = \frac{f_{\rm em} + 0.21\,(1 - f_{\rm em})}{f_{\rm em} + 0.77\,(1 - f_{\rm em})} \tag{1}$$

where 0.21 and 0.77 represent the h/e ratios of the Čerenkov and scintillator calorimeter structures, respectively. The hadron energy can be derived directly from the two signals [7]:

$$E = \frac{S - \chi C}{1 - \chi}\,, \quad \text{with} \quad \chi = \frac{\left[1 - (h/e)_S\right]}{\left[1 - (h/e)_C\right]} \approx 0.3 \tag{2}$$

The e/h values, and thus the value of the parameter χ are a bit different when lead absorber is used.

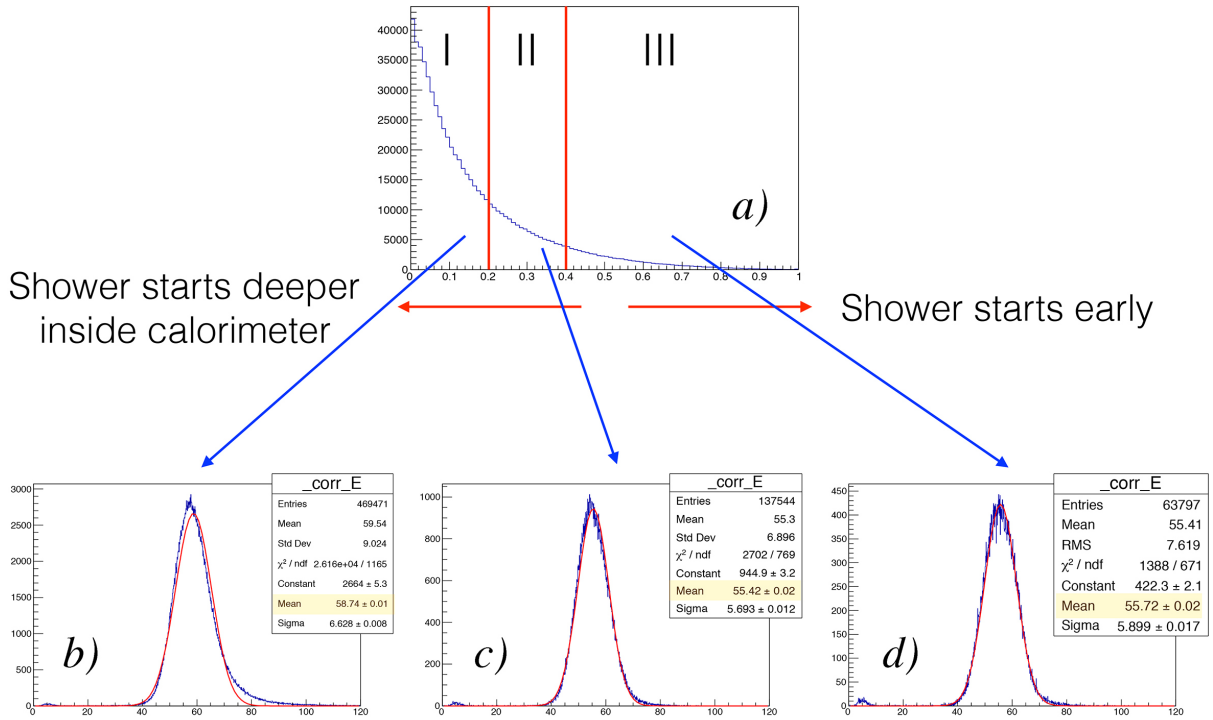

Figure 11: Signal distributions for 60 GeV π^- corrected with the dual-readout method (b,c,d), for different cuts on the fraction of the total leakage signal that was recorded in the first ring of the leakage counter array (a). See text for details.

The signal distribution for all 60 GeV π^- events shows deviations from a Gaussian shape. The type of deviations indicate that effects of light attenuation in the (scintillating) fibers are responsible for that. To investigate that, we separated the events into sub-samples, based on the fraction of the total leakage signal that was measured in the first (upstream) ring of the leakage counters. Figure 11b shows that the asymmetry is exclusively observed for events in which that fraction was small (<0.2), *i.e.* events in which most of the energy was deposited deep inside the calorimeter, where the effects of light attenuation are largest. The signal distributions for the other events are much more Gaussian (Figures 11c,d). These results indicate that light attenuation was indeed a significant factor contributing to the hadronic energy resolution of this calorimeter. As illustrated by Figure 10b, leakage fluctuations contributed the rest.

In order to investigate how effective the signals from the leakage counters were in reducing the effects of side leakage on the energy resolution, we compared the signal distributions for the 60 GeV pions in which the leakage signals were added event by event to the scintillation (Figure 12a) with the signal distributions in which the fiber scintillation signals were all multiplied with a constant factor, representing the *average* leakage fraction (Figure 12b). The leakage counters did indeed improve the hadronic energy resolution significantly, albeit not as much as one might expect from a sufficiently enlarged fiber calorimeter. It would be better to make this comparison for an event sample in which the effects of light attenuation have been reduced, *e.g.* events where more than 20% of the leakage signal is observed in the first ring of leakage counters

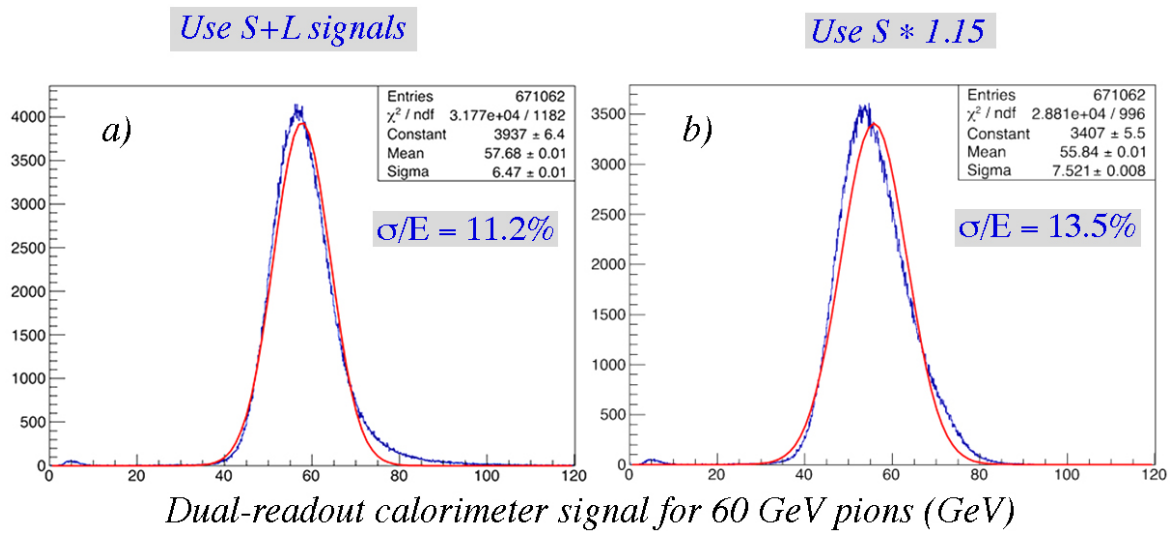

Figure 12: Signal distributions for 60 GeV π^-, corrected with the dual-readout method. The scintillation signal from the fibers was increased with the total signal measured in the leakage counters (a), or simply multiplied by a factor of 1.15 for all events (b).

(Figure 11c,d). This analysis is still a work in progress.

A second issue we wanted to investigate with the data taken during the 2015 test beam period concerned the separation of pions and protons. To that end, we used two large threshold Čerenkov counters that were installed about 50 m upstream of the calorimeter setup. These counters were filled with CO_2 gas at a pressure that was chosen depending on the beam energy. Protons were defined as particles that produced a signal compatible with the pedestal in both upstream Threshold Čerenkov counters. Pions were required to produce a signal significantly (at least 3σ) above pedestal in at least one of these counters. Figure 13 shows the signal distributions measured for beams of +40 GeV and +100 GeV. At the highest energies, these counters were not 100% efficient in separating protons from pions, but at 80 GeV, for which some results are shown in Figure 14, ineffciencies of the combined signals from the threshold Čerenkov counters were estimated to be less than 3%. A comparison of Figures 14a and 14b confirms the differences reported earlier between the em shower components of pion and proton induced hadron showers [8]. In prototype studies of the Forward Calorimeter for CMS, which is based on the detection of Čerenkov light, it was found that the signals from pions were typically $\sim 10\%$ larger than those from protons of the same energy. On the other hand, event-to-event fluctuations in these signals were $\sim 10\%$ smaller for protons, and the signal distributions were more symmetric for protons as well. Our data are in agreement with these results, which are a consequence of the requirement of baryon number conservation, which prohibits a π^0 from being the leading particle in proton induced showers. A comparison between Figures 14c and 14d shows that application of the dual-readout method (Equations 1,2) largely eliminates the differences between these two types of showers. As before, analyses of this type are likely to benefit from using an event sample in which light attenuation effects do not play a significant role. To be continued.

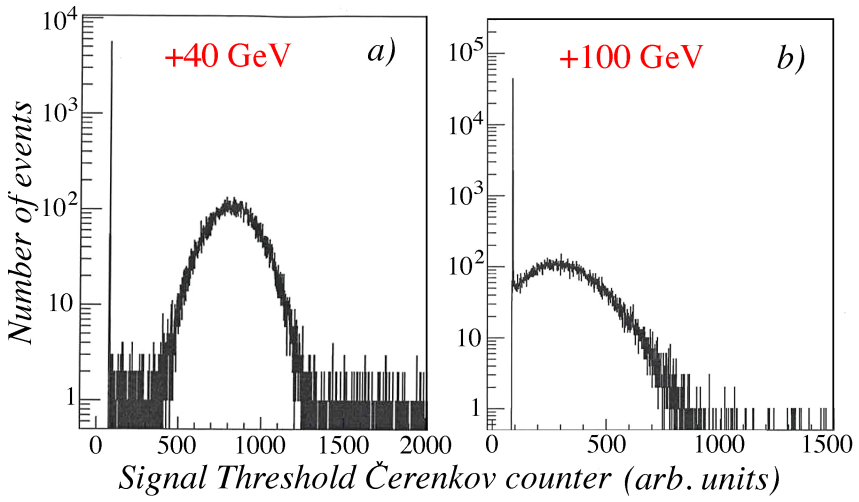

Figure 13: Signal distributions in one of the Threshold Čerenkov counters for positive particles of 40 GeV (a) and 100 GeV (b). The gas pressure was such that protons would *not* produce a signal, but pions would.

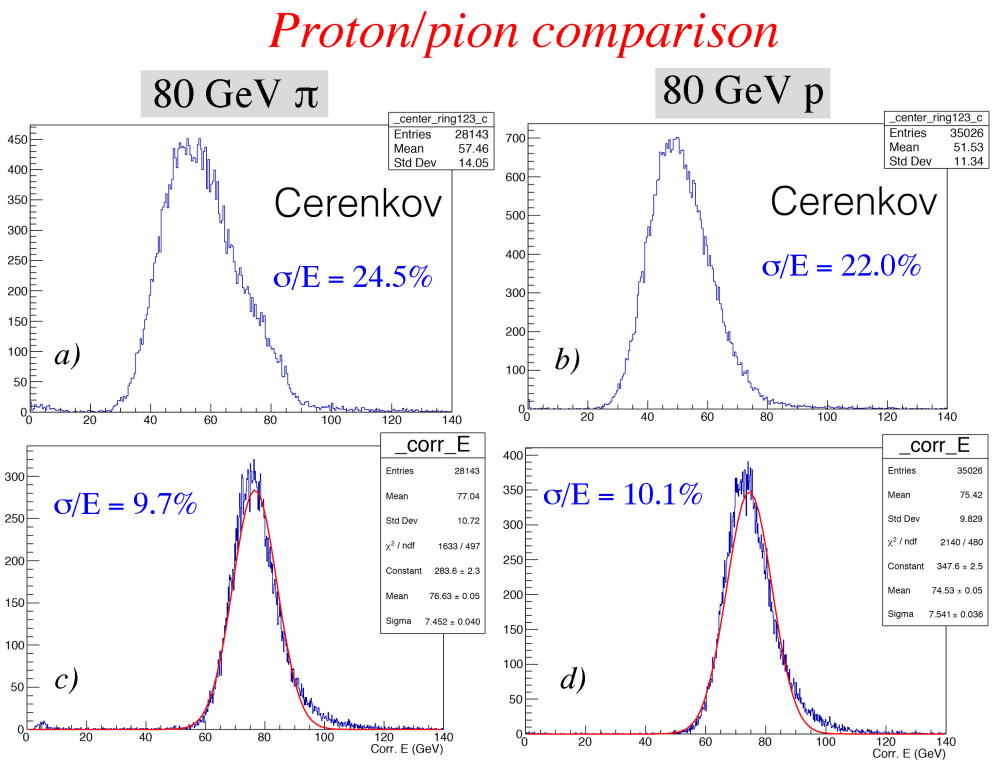

Figure 14: Signal distributions for 80 GeV pions and protons measured with the 9-module lead-based fiber calorimeter. Shown are the distributions for the Čerenkov signals from 80 GeV π^+ (a) and protons (b), as well as the dual-readout corrected total signals for 80 GeV π^+ (c) and protons (d).

A paper containing these and some other results of these measurements is in preparation, and will later this year be submitted to Nuclear Instruments and Methods for publication.

- *Hadron detection with a dual-readout fiber calorimeter*,
  S. Lee *et al.*, to be submitted to Nucl. Instr. and Meth.

3 Future plans

The DREAM/RD52 Collaboration has a very solid record of turning SPS beam time combined with limited funding into high-quality, well-regarded publications. So far, this project has resulted in 29 papers in the journal Nuclear Instruments and Methods in Physics Research, with two additional papers in preparation [9]. There is also no shortage of new ideas to further investigate the possibilities and limitations of this exciting new calorimeter concept and to optimize applications in practical detectors based on its principles. Yet, we have to face the reality that it is exceedingly difficult to obtain financial support for this type of generic detector R&D. Until now, our main sources of funding have been the US Department of Energy, through a special program for Advanced Detector Research, and INFN in Italy. However, both funding streams have dried up, because of limited resources and shifting priorities within the funding agencies[7].

For this reason, the RD52 Collaboration has now been reduced to a "coalition of the willing", a group of researchers who have been involved in the project since a long time, and who enjoy working with each other on exciting and rewarding research, in some cases at great personal expense and sacrifice. This new situation implies that we have to be realistic concerning the long-term plans outlined in a previous progress report [10]. Development of higher-density and projective absorber structures will require substantial amounts of new money, and have been put on a backburner.

One of the most challenging aspects of building this type of calorimeter is the problem of how to get very large numbers of optical fibers embedded in a uniform way in the metal absorber structure. Copper, which is the most desirable absorber for dual-readout calorimetry, has turned out to be a particular difficult material to work with. We have tried many different ways, but so far only machining grooves in thin copper plates has provided the desired quality. The existing 120-kg maximum-fiber-density copper calorimeter was built this way. Rolling copper plates has been abandoned, because of the problems with work hardening.

Professor Hauptman, who is in charge of this component of our program, works tirelessly with his colleagues at Iowa State University and the engineers of Ames National Lab to find a solution to this problem. At the present time, a combination of removing copper atoms with a water jet, followed by precison rolling of the grooves formed this way, is considered a promising venue. As an alternative, skiving is being tried as well. We are hopeful that this work will soon lead to grooved copper sheets that meet the tight tolerances needed for the construction of a sizable calorimeter module. If that is the case, we will use our remaining funds to build the largest module we can afford, reusing the PMTs from the previous (current) generation of detectors. Professor Hauptman and his crew of ISU students are ready to take on this job, which will expectedly take about 6 months to complete. While waiting for the copper production to succeed, they have also carried out a variety of other projects intended to improve the optical

[7] Recently, our Korean colleagues have managed to obtain funding for RD52, in the context of the Basic Science Research Program of the National Research Foundation of Korea (NRF).

Right edge of plate 2 sliced into four pieces in depth of roll

Figure 15: The edge of a 28 cm wide copper plate, into which grooves have been made with a combination of a water jet and precision rolling. After this procedure, the 35 cm long plate was cut into four pieces, representing different depth segments, which are shown here.

quality of this new calorimeter. One such improvement concerns mirroring the upstream ends of the fibers, which will increase the light yield and the effective attenuation length of the fibers.

In the meantime, we are preparing for the October 2016 beam tests with a program based on our existing calorimeter modules. One of the towers of the existing copper modules will be equipped with SiPM readout, since this offers the possibility to eliminate the forests of optical fibers that stick out at the rear end. These fiber bunches occupy precious space and act as antennes for particles that comes from other sources than the showers developing in the calorimeters. Tests of this new readout is part of the experimental program foreseen for this Fall.

Now that we have demonstrated that we can clearly separate the positive particle beams into proton and pion components, we would also like to see if it is possible to use the time structure of the calorimeter signals to that end. Pion showers typically carry large em components in the early stages, and this should lead to a different time structure of the signals than for protons. We are planning to use the MCP-PMTs, combined with DRS based time digitizers for these studies.

References

[1] DREAM Collaboration (Wigmans R) 2010, CERN-SPSC-2010-012/SPSC-M-771.

[2] DREAM Collaboration (Wigmans R) 2015, CERN-SPSC-2015-015/SPSC-SR-160.

[3] Cardini A *et al.* 2015, *The small-angle performance of a dual-readout fiber calorimeter*, Nucl. Instr. and Meth. in Phys. Res. **A808** (2016) 41 - 53.

[4] Akchurin N *et al.* 2014, *Lessons from Monte Carlo simulations of the performance of a dual-readout fiber calorimeter*, Nucl. Instr. and Meth. in Phys. Res. **A762** (2014) 100 - 118.

[5] Ritt S. *et al.* 2010, Nucl. Instr. and Meth. in Phys. Res. **A623** (2010) 486.

[6] Akchurin N. *et al.* 2005, Nucl. Instr. and Meth. in Phys. Res. **A537** (2005) 537.

[7] Groom D.E. 2007, Nucl. Instr. and Meth. in Phys. Res. **572** (2007) 633.

[8] Akchurin N *et al.*1998, Nucl. Instr. and Meth. in Phys. Res. **A408** (1998) 380.

[9] http://highenergy.phys.ttu.edu/dream/results/publications/publications.html

[10] DREAM Collaboration (Gaudio G, Hauptman J and Wigmans R) 2014, CERN-SPSC-2014-010 ; SPSC-SR-135.